

Review

Renal Perfusion, Oxygenation and Metabolism: The Role of Imaging

Johanna Päivärinta ¹, Ioanna A. Anastasiou ², Niina Koivuviita ¹, Kanishka Sharma ³, Pirjo Nuutila ^{4,5}, Ele Ferrannini ⁶, Anna Solini ⁷ and Eleni Rebelos ^{4,8,*}

- ¹ Department of Medicine, Division of Nephrology, Turku University Hospital, 20521 Turku, Finland; johanna.paivarinta@tyks.fi (J.P.); niina.koivuviita@tyks.fi (N.K.)
- ² 1st Department of Propaedeutic and Internal Medicine, Medical School, National and Kapodistrian University of Athens, Laiko General Hospital, 11527 Athens, Greece; anastasiouiwanna@gmail.com
- ³ Department of Imaging, Infection, Immunity and Cardiovascular Disease, University of Sheffield, Sheffield S10 2TN, UK; kanishka.sharma@sheffield.ac.uk
- ⁴ Turku PET Centre, 20521 Turku, Finland; pirjo.nuutila@utu.fi
- ⁵ Department of Endocrinology, Turku University Hospital, 20521 Turku, Finland
- ⁶ CNR, Institute of Clinical Physiology, 56124 Pisa, Italy; eleferrannini@gmail.com
- ⁷ Department of Surgical, Medical, Molecular and Critical Area Pathology, University of Pisa, 56124 Pisa, Italy; anna.solini@unipi.it
- ⁸ Department of Clinical and Experimental Medicine, University of Pisa, 56124 Pisa, Italy
- * Correspondence: eleni.rebelos@utu.fi

Abstract: Thanks to technical advances in the field of medical imaging, it is now possible to study key features of renal anatomy and physiology, but so far poorly explored due to the inherent difficulties in studying both the metabolism and vasculature of the human kidney. In this narrative review, we provide an overview of recent research findings on renal perfusion, oxygenation, and substrate uptake. Most studies evaluating renal perfusion with positron emission tomography (PET) have been performed in healthy controls, and specific target populations like obese individuals or patients with renovascular disease and chronic kidney disease (CKD) have rarely been assessed. Functional magnetic resonance (fMRI) has also been used to study renal perfusion in CKD patients, and recent studies have addressed the kidney hemodynamic effects of therapeutic agents such as glucagon-like receptor agonists (GLP-1RA) and sodium-glucose co-transporter 2 inhibitors (SGLT2-i) in an attempt to characterise the mechanisms leading to their nephroprotective effects. The few available studies on renal substrate uptake are discussed. In the near future, these imaging modalities will hopefully become widely available with researchers more acquainted with them, gaining insights into the complex renal pathophysiology in acute and chronic diseases.

Keywords: positron emission tomography; functional magnetic resonance imaging; renal perfusion; renal oxygenation; renal substrate uptake



Citation: Päivärinta, J.; Anastasiou, I.A.; Koivuviita, N.; Sharma, K.; Nuutila, P.; Ferrannini, E.; Solini, A.; Rebelos, E. Renal Perfusion, Oxygenation and Metabolism: The Role of Imaging. *J. Clin. Med.* **2023**, *12*, 5141. <https://doi.org/10.3390/jcm12155141>

Academic Editors: Anna Caroli and Nicholas Selby

Received: 21 May 2023

Revised: 2 August 2023

Accepted: 3 August 2023

Published: 6 August 2023



Copyright: © 2023 by the authors. Licensee MDPI, Basel, Switzerland. This article is an open access article distributed under the terms and conditions of the Creative Commons Attribution (CC BY) license (<https://creativecommons.org/licenses/by/4.0/>).

1. Introduction

Chronic kidney disease (CKD) is a global health burden [1] associated with unfavorable clinical and economic effects [2]. Early diagnosis is fundamental for preventing and delaying the progression of CKD [2]. Hypertension and type 2 diabetes (T2D) are leading causes of CKD while obesity and dyslipidemia have also been associated with an increased risk of CKD [3–6]. In particular, diabetic kidney disease (DKD) develops in about 30% of patients with T2D, nowadays representing the leading cause of end-stage renal disease (ESRD), and accounting for approximately 50% of all cases [7].

According to the chronic hypoxia hypothesis, renal tissue hypoxia is a unifying factor in the progression of CKD irrespective of its cause [8]. Hypoxia is associated with inflammation, vasoconstriction, vascular rarefaction, and tissue damage [9]. Given that tissue

hypoxia contributes to both CKD and acute kidney injury (AKI), understanding the causes of tissue hypoxia is of paramount clinical importance.

No more than a decade ago, inhibitors of the renin-angiotensin system (RAS), i.e., angiotensin-converting enzyme inhibitors (ACEi) or angiotensin II receptor blockers (ARB), were the only available agents that were able to reduce albuminuria. Numerous clinical trials (the Collaborative Study Group (CSG) Captopril [10], the Angiotensin II Antagonist Losartan (RENAAL) [11], the irbesartan Microalbuminuria Study (IRMA)-2 and the Irbesartan Diabetic Nephropathy Trial (IDNT) trials [12,13]) have shown the ability of these treatments to limit albuminuria and slow the glomerular filtration rate of (GFR) decline. According to a Cochrane systematic review in 2006, taking an ACE inhibitor or an ARB was associated with a statistically significant lower risk of developing ESRD compared to a placebo (relative risk (RR): 0.60; 95% CI: 0.39–0.93, respectively) and macroalbuminuria (RR: 0.45; 95% CI: 0.29–0.69) [14].

The introduction of sodium-glucose co-transporter 2 inhibitors (SGLT2-i) in clinical practice changed the treatment of both DKD and CKD in non-diabetic individuals. After attracting the attention of the medical community for their impressive reduction in mortality and cardiovascular events [15], subsequent analyses showed that SGLT2-i exerts marked renal protective effects. Dedicated kidney outcome randomised controlled trials (RCT) (CREDENCE, DAPA-CKD, and EMPA-KIDNEY) reported reduced rates in composite renal outcomes, which was defined as the doubling of serum creatinine, end-stage renal disease or renal death in patients treated with SGLT2-i [16–18].

GLP-1 RA have also been shown to reduce albuminuria. A recent meta-analysis of seven RCTs showed that their treatment with GLP-1 RA reduced the risk of a combined kidney outcome compared to a placebo (HR: 0.83; 95% CI: 0.78–0.89) [19].

Finally, finerenone, a new highly selective nonsteroidal mineralocorticoid receptor antagonist (MRA), has also yielded promising results in terms of renal protection and decreasing albuminuria in a dose-dependent manner in a cohort of patients with T2D and CKD treated with RAS blockage [20,21]. Moreover, the Figaro-DKD trial showed that the kidney composite outcome (ESRD, a sustained $\geq 57\%$ decrease in eGFR from baseline for ≥ 4 weeks, or renal death) occurred less frequently in the finerenone group compared to the placebo (HR: 0.77; 95% CI: 0.60–0.99) [21]. Currently, at least one RCT evaluated whether the combination of finerenone with SGLT2-i had additive effects on renal outcomes [22] (ClinicalTrials.gov Identifier: NCT05254002).

In parallel with the quick improvement in the medical “arsenal” for halting the progression of CKD, the last few years have seen important progress in the field of medical imaging, enabling the *in vivo* study of renal pathophysiology in humans. Moreover, a multidisciplinary European network (European Cooperation in Science and Technology Action, PARENCHIMA) has been created that aims to disseminate the clinical use of renal MRI biomarkers. The various available MRI techniques and their main clinical/research applications were described in the position paper of PARENCHIMA [23], along with their technical recommendations [24].

In this narrative review, we focus on studies assessing renal perfusion (arterial spin labelling (ASL), magnetic resonance imaging (MRI), positron emission tomography (PET), renal oxygenation (blood oxygenation level-dependent (BOLD) MRI) and metabolism (PET), a triad of physiologic determinants of kidney function, which have so far not been extensively investigated in humans. Special interest has also been given to studies where the effects of SGLT2-i on renal physiology have been assessed. Other imaging modalities are extensively described elsewhere [23,25,26].

1.1. Renal Perfusion

Despite comprising $<1\%$ of body weight, the kidneys receive a high blood flow (~ 1.2 – 1.4 L/min), which accounts for $\sim 20\%$ of the cardiac output in the resting adult in the face of a small total kidney mass (300 gr). The kidneys have a unique perfusion system with two separate capillary beds, while the renal cortex receives a large blood flow:

only 10% of renal blood flow perfuses the renal medulla, with evidence that cortical and medullary circulations are independently regulated [27]. Even in healthy subjects, the medulla appears to operate under conditions of quasi-hypoxia. The coupling between perfusion, oxygenation, and metabolism is complex and not completely understood. A preclinical study in rabbits showed that renal tissue PO_2 is independent of the renal blood flow (RBF) because the preglomerular diffusional shunting of oxygen from the arteries to veins decreases with decreasing RBF and vice versa [28].

1.2. Principles of MRI-Measurement of Renal Perfusion (ASL) and Oxygenation (BOLD)

A dynamic contrast-enhanced MRI uses gadolinium for radiocontrast, which is cleared almost completely through glomerular filtration. Thus, gadolinium does not remain in the blood circulation, thereby complicating the evaluation of kidney perfusion. Furthermore, the nephrogenic systemic fibrosis that is associated with gadolinium use in patients with CKD mandates the cautious rational use of gadolinium. Ultrasmall superparamagnetic iron oxide particles like ferumoxytol have been introduced as kidney-safe MRI contrast agents [29].

A fairly new MRI method to study renal perfusion is arterial spin labelling (ASL), which utilises radiofrequency (RF) pulses to alter the longitudinal magnetisation of water in the blood into a diffusible endogenous tracer [30]. A flow-sensitised “label” (or tag) image is acquired after a time delay to ensure the arrival of “labelled” blood to the renal tissue microvasculature. This image acquisition is then repeated to obtain a “control” image without altering the magnetisation of the inflowing blood. As the static tissue spins have the same magnetisation preparation; the difference in the signal of inflowing blood is only due to a different preparation, and subtracting the two resulting images yields a perfusion-weighted image (PWI) [31]. These PWIs are then fed into a model that describes the relationship between the difference in the signal and the actual blood perfusion. The result is a quantitative perfusion map (RBF) with units mL/100 g of tissue/min [31]. Different variants of ASL, such as continuous (CASL), pulsed (PASL), and pseudo-continuous (PCASL) [32,33], can be used to invert the arterial blood magnetization and obtain the renal tissue’s perfusion. Figure 1 shows an example of the ASL perfusion weighted image (left panel) and the resulting renal blood flow map (right panel) using the CASL technique.

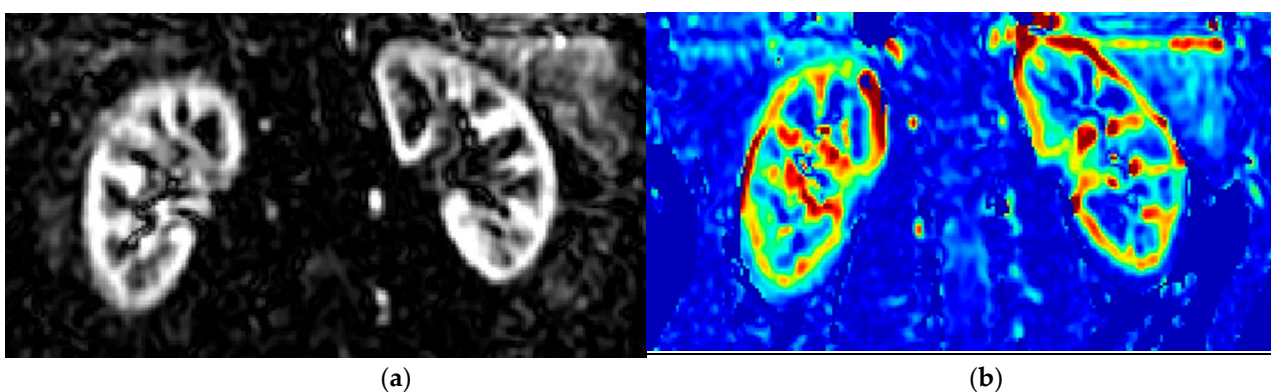


Figure 1. Representative perfusion weighted image (a) and the resulting RBF map (b) from the renal ASL (CASL) MRI technique on a healthy volunteer.

BOLD imaging is another MRI sequence that allows the measurement of renal oxygenation. In principle, this sequence uses the paramagnetic properties of deoxyhemoglobin to assess tissue oxygenation. This measurement yields the relaxation rate $R2^*$, which is proportional to deoxyhemoglobin levels: i.e., the higher the $R2^*$, the lower the oxygenation. In a typical BOLD-fMRI study, the renal parenchyma is divided into 12 layers of equal thickness; the outer three layers are considered indicative of renal cortex oxygenation,

whereas values from the 8th to 10th layer are representative of the medullary region. Other than evaluating the $R2^*$, the slope of the linear part of the regression of the $R2^*$ values on the depth of the renal parenchyma (0% at the outer layer to 100% at the inner layer) can be used to express the oxygenation results [34].

1.3. Renal Perfusion and Renal Oxygenation Using MRI

Several studies have assessed renal perfusion using ASL [30] and oxygenation using BOLD MRI [35]. In an elegant study by Prasad and colleagues, patients with CKD and control subjects were studied with ASL, BOLD, and diffusion MRI. Renal cortical perfusion was reduced in CKD subjects compared to the controls (109.54 ± 25.38 vs. 203.17 ± 27.47 mL/min/100 g; $p < 0.001$); however, there was no difference in cortical oxygenation, nor were oxygenation or perfusion related to each other. However, as the authors discussed, it is unknown whether oxygenation is decreased in patients with CKD, as BOLD MRI might not be sufficiently sensitive to detect subtle deficits [36].

Zanchi et al. studied the acute and chronic effects of 10 mg empagliflozin in 45 healthy volunteers with $eGFR > 60$ mL/min/1.73 m² and normoalbuminuria; in these healthy volunteers, SGLT2-i did not induce any acute or chronic effects on cortical and medullary oxygenation [37]. In a placebo-controlled cross-over trial, 15 patients with type 1 diabetes (T1D) received a single administration of dapagliflozin with 50 mg or a placebo; compared to the placebo, treatment with dapagliflozin improved renal cortical oxygenation, while it did not affect perfusion [38]. The authors suggested that this increase in cortical oxygenation could be attributed to a reduced tubular transport workload in the proximal tubules. The eventual beneficial effects of SGLT2-i on renal oxygenation were, however, unconfirmed in a recent study assessing the chronic effects of SGLT2-i on renal oxygenation and perfusion. In particular, the effects of semaglutide (a GLP-1 RA) and empagliflozin or their combination for 32 weeks were assessed by Gullaksen and colleagues. Semaglutide decreased cortical and medullary perfusion, whereas empagliflozin did not affect kidney perfusion while decreasing medullary oxygenation [39]. When both drugs were combined, medullary oxygenation and renal perfusion declined [39]. The authors concluded that the nephroprotective effects of SGLT2-i were probably not due to an improvement in medullary oxygenation [39]. However, to the best of our knowledge, kidney perfusion before and after treatment with SGLT2-i has not been thus far studied with PET, and it would be relevant to assess the acute and chronic effects of these new drugs on renal perfusion and oxidative metabolism.

Lastly, in an elegant study, Pruijm and colleagues [34] measured cortical oxygenation in patients with CKD and in healthy controls. Patients with CKD showed decreased cortical oxygenation, and at 3 years of follow-up, those who at the baseline had a higher outer $R2^*$ or a flat $R2^*$ slope had a three-fold higher risk for renal replacement therapy or a $>30\%$ increase in serum creatinine [34].

1.4. Basics of PET and Renal Cortical Perfusion

To measure renal perfusion, the blood volume that passes through a unit mass of renal tissue in a given time ($\text{mL} \cdot \text{g}^{-1} \cdot \text{min}^{-1}$) must be quantified. The signal intensity changes within the abdominal aorta; therefore, an arterial input function is needed when quantitative parameters are measured. Semi-quantitative measurements of renal perfusion only require recording signal intensity changes within the kidney. Quantitative imaging methods are able to give regional renal perfusion instead of only whole-kidney perfusion [40].

Like ASL MRI, positron emission tomography (PET) provides a non-invasive quantitative method to study renal regional perfusion. The PET signal detection generates three-dimensional images in which each voxel provides an estimate of the radionuclide concentration within the volume of tissue represented by that voxel. There is no need for a contrast agent, and the amount of ionizing radiation is minimal. Thus, PET is a safe and promising method for studying renal perfusion in patients with CKD.

For the PET assessment of renal cortical perfusion, a positron-emitting radiopharmaceutical that traces renal perfusion is required. PET exploits the physics of positron-electron annihilation when localizing the site of the positron decay inside the patient's body. As a result of annihilation, a pair of photons is detected outside the patient's body by gamma detectors [41]. Correction for decay, dead time, and photon attenuation is needed. The distribution of the positron-emitting tracer in the kidney can be reconstructed to a three-dimensional image by mathematical algorithms. Perfusion quantification after the intravenous administration of a tracer demands the application of compartmental models describing the relationship between tissue count rates and the rate of regional perfusion. The conversion of the imaged tissue count rates into absolute numeric values of perfusion also requires knowledge of the quantity of the tracer in the arterial blood. Since an arterial input function (i.e., the concentration of the radioactive tracer in the blood over time) is needed for the analysis of PET data, these data can be obtained either by frequent arterial or "arterialised" blood sampling or by "extracting" the arterial input function directly from the PET data. The latter can be obtained by drawing small regions of interest in the aorta or within the left ventricle cavity [41]. PET provides only moderate spatial resolution, and this leads to a partial volume effect that causes the overestimation or underestimation of perfusion.

1.5. Tracers in Renal Perfusion PET

An optimal perfusion tracer should show complete and perfusion-rate-independent extraction from arterial blood during its first pass transit through the renal capillaries [41].

The most widely used tracer to assess perfusion is [^{15}O]H₂O, which is an inert and freely diffusible tracer already used in several PET-based studies to evaluate renal perfusion. One-compartment or two-compartment kinetic models have been used for [^{15}O]H₂O-PET [41]. Although in our centre, as in others, this is the most widely used tracer to assess perfusion, its short half-life (2 min) of [^{15}O] necessitates a nearby cyclotron and, thus, limits its wider availability. In addition, the reversible binding and fast dynamics of the [^{15}O]H₂O tracer are technically error-prone due to the relatively low temporal resolution of PET [41].

Kidney perfusion measured with the gold standard method of para-aminohippuric acid (PAH) clearance and [^{15}O]H₂O-PET-based kidney perfusion is directly related to each other in both healthy subjects and in patients with CKD [42,43]. Moreover, renal cortical perfusion measured by [^{15}O]H₂O-PET has been shown to correlate with estimated GFR (eGFR) [44].

[^{13}N]-ammonia (half-life of 10 min) has an extraction fraction that varies with the rate of perfusion, and it is neither freely diffusible nor inert. However, the 10 min half-life of [^{13}N]-ammonia and its prolonged retention in the kidney allow extended image acquisition periods, thereby improving the data and image quality [41]. Limitations of the [^{13}N]-ammonia approach include the need to correct for [^{13}N]-ammonia-metabolites in the blood, and the instability of the model at both very high and very low perfusion levels, resulting in the high coefficients of variation in renal perfusion estimates [41]. A linear correlation between [^{15}O]H₂O-PET and [^{13}N]-ammonia-PET-based renal cortical perfusion has been reported [45].

[^{11}C]-acetate (half-life of 20 min) can assess both kidney perfusion and kidney oxygen consumption. [^{11}C]-acetate- and [^{15}O]H₂O-PET-based renal cortical perfusion correlate with each other [46].

[^{82}Rb]-Chloride (half-life of 75 s) has also been used to assess renal perfusion, with some studies suggesting that [^{82}Rb]-chloride-PET can measure effective renal plasma flow [47].

The PET studies that have assessed renal cortical perfusion are presented in Table 1.

1.6. Clinical Settings Where Renal Perfusion Has Been Assessed with PET

In healthy subjects, the values of renal cortical perfusion measured with [^{15}O]H₂O-PET have ranged from 1.6 mL·g⁻¹·min⁻¹ to 4.7 mL·g⁻¹·min⁻¹ (Table 1). [^{15}O]H₂O-PET

studies have shown reduced renal cortex perfusion in patients with CKD compared to healthy subjects [43,48] and decreasing values through CKD stages (2.2 mL·g⁻¹·min⁻¹ in CKD stage 3 [42], 2.1 mL·g⁻¹·min⁻¹ in CKD stage 3–4 [42], and 1.3 mL·g⁻¹·min⁻¹ in CKD 4–5) [48].

In the only [¹⁵O]H₂O-PET study performed thus far in kidney transplant recipients (N = 19, median time from transplantation 33 months; eGFR 55mL/min), renal cortical perfusion was compared to healthy controls [44]. No statistically significant difference emerged in renal cortical perfusion between the two groups [2.2 (2.0–3.0) mL·g⁻¹·min⁻¹ vs. 2.2 (2.4–4.0) mL·g⁻¹·min⁻¹ for patients and healthy controls, respectively, with the median (IQR)]; however, kidney transplant recipients had higher renal vascular resistance (mean arterial pressure/renal cortical perfusion) compared to the controls [44].

Three studies have evaluated renal cortical perfusion in patients with other diseases than CKD. In the study of Assersen et al., there was no difference in the renal cortical perfusion values measured by [¹⁵O]H₂O-PET between patients with hypertension and no CKD and healthy controls [49]. In patients with morbid obesity, when compared to healthy lean subjects, there were no differences in cortical or medullary perfusion per unit of tissue mass (mL/min/100 g of tissue). However, when accounting for kidney volume, obese individuals received a higher total renal blood flow (mL/min) compared to lean controls [50]. In that study, patients who underwent bariatric surgery and renal perfusion measurements repeated after major weight loss showed a significant reduction in the total renal blood flow [50]. Lastly, renal cortical perfusion has also been assessed in patients with heart failure: such patients receive a lower blood flow to the renal cortex compared to healthy controls [51].

Table 1. Renal cortical perfusion in PET studies.

Reference	N and Type of Subjects	Tracer	Cortex Perfusion (mL·g ⁻¹ ·min ⁻¹)
Nitzsche et al., 1993 [45]	20 healthy subjects	[¹⁵ O]H ₂ O	4.7 (0.3)
		[¹³ N]-ammonia	4.6 (0.5)
Middlekauff et al., 2001 [51]	29 healthy subjects	[¹⁵ O]H ₂ O	4.4 (0.1)
Middlekauff et al., 1997 [52]	19 healthy subjects	[¹⁵ O]H ₂ O	4.2 (0.1)
	19 pts with heart failure	[¹⁵ O]H ₂ O	3.0 (0.1)
Alpert et al., 2002 [43]	5 healthy subjects	[¹⁵ O]H ₂ O	3.4 (0.4)
	10 pts with renal disease	[¹⁵ O]H ₂ O	2.1 (1.1)
Juillard et al., 2002 [42]	8 pts with CKD	[¹⁵ O]H ₂ O	2.2 (2.0)
Kudomi et al., 2009 [53]	6 healthy subjects	[¹⁵ O]H ₂ O	1.6 (0.6) *
			3.6 (2.2)
Damkjær et al., 2010 [54]	9 healthy subjects	[¹⁵ O]H ₂ O	4.7 (0.3)
Damkjær et al., 2012 [55]	7 healthy subjects	[¹⁵ O]H ₂ O	3.6 (0.1)
Assersen et al., 2019 [49]	12 healthy subjects	[¹⁵ O]H ₂ O	
	6 pts with hypertension	[¹⁵ O]H ₂ O	4.1 (0.3)
Rebelos et al., 2019 [50]	15 healthy subjects	[¹⁵ O]H ₂ O	2.7 (104)
	23 women with obesity	[¹⁵ O]H ₂ O	2.6 (62)
	10 healthy subjects		1.8 (0.3)
Koivuviita et al., 2012 [48]	7 pts with CKD	[¹⁵ O]H ₂ O	1.26 (0.5)
	17 pts with RAS and CKD		1.43 (0.4)
Päivärinta et al., 2019 [44]	10 healthy subjects	[¹⁵ O]H ₂ O	2.7 (2.4–4.0)
	19 pts with kidney Tx	[¹⁵ O]H ₂ O	2.2 (2.0–3.0)
Normand et al., 2019 [46]	10 healthy subjects	[¹⁵ O]H ₂ O	3.3 (0.7)
		[¹¹ C]-acetate	1.7 (0.3)

N, number of subjects. Data are mean (SD), median [IQR], median (Q2–Q3). *, renal cortical perfusion was measured based on K1 and K2, respectively. RAS, renal artery stenosis, CKD, chronic kidney disease.

1.7. Reproducibility of Renal Cortical PET Perfusion

Nitzsche et al. performed repeat measurements of renal blood perfusion using [¹³N]-ammonia PET and reported that the individual interstudy difference was 5.0% [45]. The

individual interstudy difference in [^{15}O]H $_2$ O measurements was even smaller, ~2.2%. The interstudy differences of the renal cortical blood perfusion estimates within each individual approach were insignificant [45]. In the study of Normand et al., the typical errors were 0.36 and 0.22 for [^{15}O]H $_2$ O and [^{11}C]-acetate and the interclass correlation coefficient, which were 0.64 and 0.26, respectively [46].

1.8. Assessment of Renal Metabolism Using PET

The kidney is a key metabolic player, with the ability to both produce and dispose of glucose. Gluconeogenesis takes place in the cortex and, in particular, at the proximal tubular cells (PCT), which are the only renal cells characterised by glucose-6-phosphatase activity [56]. Glucose disposal occurs both via glucose elimination in the urine and through glucose uptake and utilisation by renal cells. Cells in the cortical region use glucose and other substrates, whereas cells in the medulla predominantly rely on glucose [57]. Renal substrate uptake rates have been assessed using the arterial-venous difference technique. Currently, this invasive method is seldom used in specialised centres and has the drawback of yielding whole-organ substrate uptake values rather than differentiating between cortical and medullary substrate uptake rates. Only recently, PET has been introduced to assess renal metabolism.

We have previously shown that when using 14(R,S)-[^{18}F]Fluoro-6-thia-heptadecanoic acid ([^{18}F]FTHA) PET to study renal fatty acid uptake (FFA), the kidney (cortical and medullary) FFA uptake is higher in obese individuals compared to healthy lean controls. These patients were re-studied six months after bariatric surgery, and we observed that, despite significant weight loss and an improvement in insulin sensitivity, renal FFA uptake remained high. This might be attributed to the ongoing catabolic state and increased FFA availability [50].

We have also recently used [^{18}F]FDG-PET to assess regional kidney glucose metabolism, which has never been measured before [58]. The main problem with this approach is that [^{18}F]FDG is excreted in the urine while, in the presence of normoglycaemia, virtually all the filtered glucose is re-absorbed by SGLTs; consequently, the [^{18}F]FDG radioactivity remaining within the renal tubular space is mistakenly “read” as part of the glucose uptake by the surrounding cells. To tackle this problem, we acquired renal radioactivity data as late scans (~90 min from [^{18}F]FDG injection) to allow for most of [^{18}F]FDG excreted in the urine to be already washed out of the kidneys toward the bladder. Then, using the amount of [^{18}F]FDG excreted in the urine at the end of the PET studies, it was possible to calculate the remaining intratubular [^{18}F]FDG activity and correct the results. Through this approach, we showed that lean healthy controls had higher cortical and medullary GU rates compared to patients with obesity under both fasting and insulin clamp conditions (1 mU/kg/min). Moreover, we found that cortical, but not medullary, GU was enhanced during insulin clamp compared to the fasting study. Taken together, these data suggest that the renal cortex is an insulin-sensitive tissue [58]. Moreover, this study demonstrated that, albeit the fact that [^{18}F]FDG-PET results underestimate renal glucose uptake, this method can still yield clinically useful information regarding renal metabolism [58]. Representative images of an [^{18}F]FDG scan during the euglycemic hyperinsulinemic clamp are shown in Figure 2.

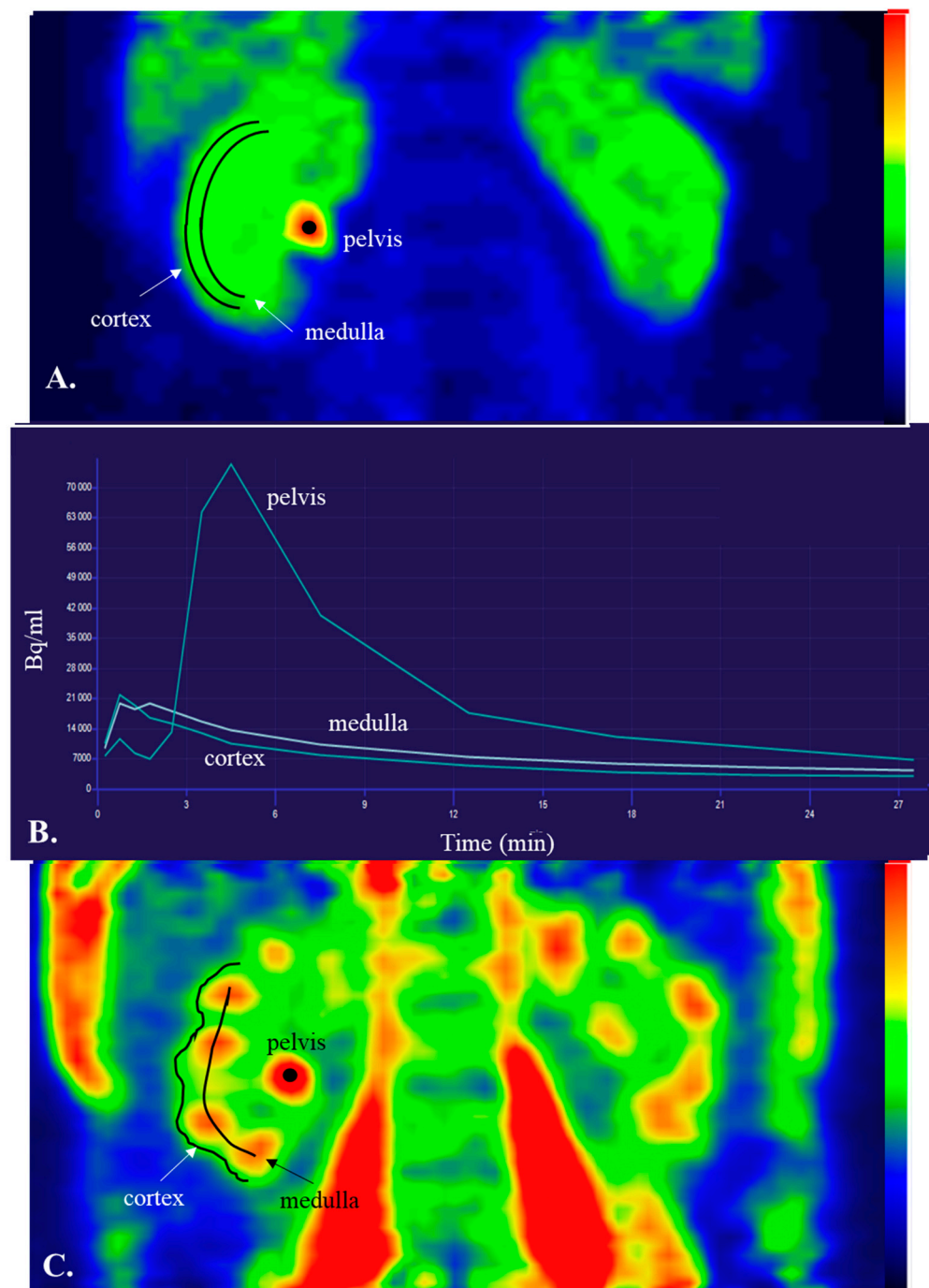


Figure 2. (A,B) Show an “early” scan immediately after [^{18}F]FDG injection and the time–activity curves in the renal cortex, medulla and pelvis. Notice that [^{18}F]FDG quickly reaches the renal pelvis (Figure 1b). (C) Shows a “late” scan acquired ~60 min after [^{18}F]FDG injection. Data from the same subject are shown.

2. Discussion

Compared to the time-honored gold standard method for assessing renal perfusion (i.e., PAH clearance), the use of imaging to assess renal perfusion provides several substantial benefits. First, imaging is less invasive (in the case of fMRI, only images are acquired, whereas in the case of PET, the most widely used tracer [^{15}O]H $_2$ O only requires the i.v. administration of the tracer, but no blood sampling). Acquisition times are also much shorter (~5 min for an [^{15}O]H $_2$ O, and ~10 min for ASL MRI [30]) compared to a standard 2 h study that is necessary for the PAH clearance method. Importantly, imaging allows for

the independent evaluation of the renal perfusion of the two kidney regions characterised by major differences in perfusion, whereas PAH only yields estimates of the total renal perfusion. The latter benefit of imaging also holds true when comparing invasive methods, such as the AV differences technique, to evaluate oxygen or substrate extraction by the kidneys, whereas PET can differentiate between the uptake rates in the cortex and the medulla, though not perfectly, as described below.

Only a few studies have used these potent imaging modalities to assess renal physiology, and most of these studies have been performed in healthy subjects. Thus far, [^{15}O]H $_2\text{O}$ is the most widely used PET tracer to assess renal perfusion (Figure 3). Overall, renal cortical perfusion measured by [^{15}O]H $_2\text{O}$ PET has given consistent results across studies; most importantly, such studies have confirmed earlier findings using PAH clearance. It is also important to underline that even though [^{15}O]H $_2\text{O}$ is the most widely used tracer to assess renal perfusion, the involved modelling is still suboptimal, and efforts are being made to improve it. [^{13}N]-ammonia also seems to be a reliable tracer for imaging renal perfusion, although there is the need to correct for [^{13}N]-ammonia metabolites in the blood, and the [^{13}N]-ammonia model is unstable at both very high and very low perfusion levels. [^{11}C]-acetate is a promising tracer because it can provide not only information regarding perfusion but also give information regarding oxidation. All these PET tracers show relatively short half-lives, thus confining their main use in PET centres with cyclotrons.

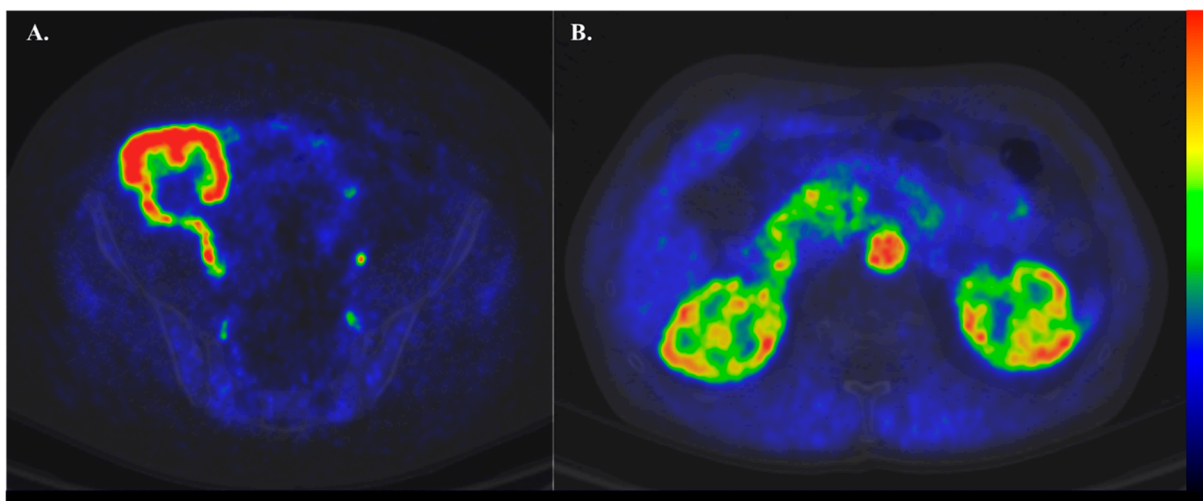


Figure 3. Representative [^{15}O]H $_2\text{O}$ -PET images of a kidney transplant patient (A) and a healthy lean control (B).

Still, there are some further methodological aspects to consider when using PET to assess both renal perfusion and renal substrate uptake rates. First, the renal cortex and renal medulla are very close areas, and due to the relatively poor spatial resolution of PET, it is not possible to completely differentiate the signal between these two structures. Apart from the spatial resolution, drawing an accurate region of interest might also be biased as it is impossible to define the border between the cortex and medulla without the use of contrast-enhanced CT or MRI. Few studies have attempted to exactly define this border. Contrast-enhanced CT was used in two studies with [^{15}O]H $_2\text{O}$ [49,55]. In the only [^{11}C]-acetate study of renal cortical perfusion, T1 weighted MRI was used to define the border between the cortex and medulla [46]. Damkjær et al. introduced a new technique to differentiate between the renal cortex and medulla: tissue layers with a thickness of one voxel were eliminated stepwise from the external surface of the volume of interest (voxel peeling) until there was no decrease in the blood perfusion and the medulla was reached [54,55]. Renal PET/MRI studies have the additional advantage of better anatomical distinction between these two regions compared to PET/CT studies and also of a lower radiation burden to the studied subjects [59].

The most novel fMRI modalities (ASL and BOLD) have also started to be used in specialised centres, with some of the latest publications focusing on the hemodynamic effects of anti-hyperglycemic agents with nephroprotective effects.

Even though BOLD fMRI is, in fact, the only non-invasive way that is currently available to assess renal oxygenation in humans, it should be kept in mind that it is not a direct measure of tissue oxygenation, as changes in the blood volume can affect the amount of deoxyhaemoglobin in the tissue. Recently, a pilot study in healthy subjects and in patients with CKD addressed this issue by combining BOLD fMRI with ferumoxytol to estimate the fractional renal tissue blood volume. With the combination of these two methods, the authors could estimate tissue oxygenation and showed that, indeed, patients with CKD had decreased StO₂ and blood PO₂ in the renal cortex and the renal medulla compared to the healthy subjects, confirming the chronic hypoxia hypothesis [60].

Currently, at the Turku PET Centre there is ongoing work to validate the use of [¹⁵O]O₂ for the assessment of renal oxygenation with PET.

When applying functional renal imaging (PET or fMRI), it should be considered that physiologic parameters might also affect kidney perfusion results, some of which might be easy and others impossible to control. It is now well-established that, before a kidney perfusion study, salt and water intake should be balanced and reported, as salt loading is associated with renal cortical vasoconstriction and decreased cortical perfusion [49]. Indeed, recent reports on this topic used standardised hydration and salt-consuming protocols before performing the studies. However, kidney cortical perfusion has also been shown to decrease during handgrip exercises and during mental stress via the activation of the sympathetic nervous system [47,51,52]. These data suggest that study participants should be put in at-ease conditions, something that might be difficult to obtain, for instance, if a subject suffers from mild claustrophobia during the imaging session. Future studies should evaluate stress hormones to correlate with the results of kidney perfusion measurements, whereas, in paired experiments, similar study conditions should be ensured on different experimental days.

From a physiologic standpoint, whether renal oxygenation and renal perfusion are directly and linearly interrelated is not known, mainly due to the difficulties in assessing these aspects in humans. Progress in medical imaging makes it possible to study aspects of renal physiology that in the past relied only on the measurement of AV differences. In this respect, renal imaging may give substantial new insights regarding the mechanisms of action of new potent nephroprotective drugs. Some investigations on the renal hemodynamic effects of SGLT2-i and GLP1-RA have already been published [39], and more research on this topic is expected.

It should be also pointed out that, so far, there are no studies in which renal cortical perfusion has been measured with both PET and an MRI. Ongoing research on the iBEAT project should clarify this aspect [61]. Considering the lower radiation burden needed in studies using ultralong field-of-view PET scanners, a combination of PET with MRI in future investigations is expected to increase our insight into the physiology of renal function and the pathophysiology of kidney diseases. Apart from the methodological considerations described above, the high costs of these imaging modalities and the need for the “on-site” production of short-lived radiotracers are important aspects that have thus far limited a broader use of renal imaging.

Our research group has been a pioneer in evaluating renal substrate uptake rates using PET. With this method, we have shown that, in the context of insulin resistance, renal FFA uptake is increased, whereas renal glucose uptake during standardised insulinisation is decreased. Future reports might further elaborate on whether an altered renal substrate uptake is associated with progressive kidney damage and whether a lifestyle modification or bariatric surgery could correct it [62], evaluating the interplay between renal metabolism and the adjacent organs, such as renal sinus fat [63], and the liver [64]. With respect to the liver, recent reports have shown that carriers of the PNPLA3 p.I148M variant (i.e., the main genetic determinant of non-alcoholic fatty liver disease) have impaired kidney function [65];

however, the mechanisms linking hepatic steatosis with a worse renal function are still partially unknown.

In conclusion, renal function imaging “is here to stay” and may provide useful insight into the physiology (perfusion, oxygenation, metabolism) of the kidney; our ultimate goal is to protect these organs from the various insults metabolic diseases and modern lifestyles impose on them.

Author Contributions: J.P., I.A.A., K.S., A.S. and E.R. drafted the manuscript. N.K., P.N. and E.F. critically revised the text. All authors have read and agreed to the published version of the manuscript.

Funding: J.P. reports funding from Academy of Finland, grant number 307402, BEAT DKD EU project. ER reports funding from the Finnish Medical Foundation and the Finnish Diabetes Research Foundation.

Institutional Review Board Statement: Not applicable.

Informed Consent Statement: Not applicable.

Data Availability Statement: Not applicable.

Acknowledgments: The authors would like to thank Vesa Oikonen, and Hidehiro Iida for useful discussions while drafting this text.

Conflicts of Interest: The authors declare no conflict of interest.

References

1. Bello, A.K.; Levin, A.; Tonelli, M.; Okpechi, I.G.; Feehally, J.; Harris, D.; Jindal, K.; Salako, B.L.; Rateb, A.; Osman, M.A.; et al. Assessment of Global Kidney Health Care Status. *JAMA* **2017**, *317*, 1864–1881. [[CrossRef](#)] [[PubMed](#)]
2. Stack, A.G.; Casserly, L.F.; Cronin, C.J.; Chernenko, T.; Cullen, W.; Hannigan, A.; Saran, R.; Johnson, H.; Browne, G.; Ferguson, J.P. Prevalence and Variation of Chronic Kidney Disease in the Irish Health System: Initial Findings from the National Kidney Disease Surveillance Programme. *BMC Nephrol.* **2014**, *15*, 185. [[CrossRef](#)] [[PubMed](#)]
3. Collins, A.J.; Foley, R.N.; Chavers, B.; Gilbertson, D.; Herzog, C.; Johansen, K.; Kasiske, B.; Kutner, N.; Liu, J.; St Peter, W.; et al. United States Renal Data System 2011 Annual Data Report: Atlas of Chronic Kidney Disease & End-Stage Renal Disease in the United States. *Am. J. Kidney Dis.* **2012**, *59*, e1–420.
4. Muntner, P.; Coresh, J.; Smith, J.C.; Eckfeldt, J.; Klag, M.J. Plasma Lipids and Risk of Developing Renal Dysfunction: The Atherosclerosis Risk in Communities Study. *Kidney Int.* **2000**, *58*, 293–301. [[CrossRef](#)]
5. Lin, T.-Y.; Liu, J.-S.; Hung, S.-C. Obesity and Risk of End-Stage Renal Disease in Patients with Chronic Kidney Disease: A Cohort Study. *Am. J. Clin. Nutr.* **2018**, *108*, 1145–1153. [[CrossRef](#)]
6. Moriconi, D.; Antonioli, L.; Masi, S.; Bellini, R.; Pellegrini, C.; Rebelos, E.; Taddei, S.; Nannipieri, M. Glomerular Hyperfiltration in Morbid Obesity: Role of the Inflammasome Signalling. *Nephrology* **2022**, *27*, 673–680. [[CrossRef](#)] [[PubMed](#)]
7. Tuttle, K.R.; Bakris, G.L.; Bilous, R.W.; Chiang, J.L.; de Boer, I.H.; Goldstein-Fuchs, J.; Hirsch, I.B.; Kalantar-Zadeh, K.; Narva, A.S.; Navaneethan, S.D.; et al. Diabetic Kidney Disease: A Report from an ADA Consensus Conference. *Am. J. Kidney Dis.* **2014**, *64*, 510–533. [[CrossRef](#)]
8. Fine, L.G.; Norman, J.T. Chronic Hypoxia as a Mechanism of Progression of Chronic Kidney Diseases: From Hypothesis to Novel Therapeutics. *Kidney Int.* **2008**, *74*, 867–872. [[CrossRef](#)]
9. Chade, A.R. Small Vessels, Big Role: Renal Microcirculation and Progression of Renal Injury. *Hypertension* **2017**, *69*, 551–563. [[CrossRef](#)]
10. Lewis, E.J.; Hunsicker, L.G.; Bain, R.P.; Rohde, R.D. The Effect of Angiotensin-Converting-Enzyme Inhibition on Diabetic Nephropathy. The Collaborative Study Group. *N. Engl. J. Med.* **1993**, *329*, 1456–1462. [[CrossRef](#)]
11. Brenner, B.M.; Cooper, M.E.; de Zeeuw, D.; Keane, W.F.; Mitch, W.E.; Parving, H.H.; Remuzzi, G.; Snapinn, S.M.; Zhang, Z.; Shahinfar, S. Effects of Losartan on Renal and Cardiovascular Outcomes in Patients with Type 2 Diabetes and Nephropathy. *N. Engl. J. Med.* **2001**, *345*, 861–869. [[CrossRef](#)]
12. Parving, H.H.; Lehnert, H.; Bröchner-Mortensen, J.; Gomis, R.; Andersen, S.; Arner, P. The Effect of Irbesartan on the Development of Diabetic Nephropathy in Patients with Type 2 Diabetes. *N. Engl. J. Med.* **2001**, *345*, 870–878. [[CrossRef](#)] [[PubMed](#)]
13. Lewis, E.J.; Hunsicker, L.G.; Clarke, W.R.; Berl, T.; Pohl, M.A.; Lewis, J.B.; Ritz, E.; Atkins, R.C.; Rohde, R.; Raz, I. Renoprotective Effect of the Angiotensin-Receptor Antagonist Irbesartan in Patients with Nephropathy Due to Type 2 Diabetes. *N. Engl. J. Med.* **2001**, *345*, 851–860. [[CrossRef](#)] [[PubMed](#)]
14. Strippoli, G.F.M.; Bonifati, C.; Craig, M.; Navaneethan, S.D.; Craig, J.C. Angiotensin Converting Enzyme Inhibitors and Angiotensin II Receptor Antagonists for Preventing the Progression of Diabetic Kidney Disease. *Cochrane Database Syst. Rev.* **2006**, *2006*, CD006257. [[CrossRef](#)] [[PubMed](#)]

15. Zinman, B.; Wanner, C.; Lachin, J.M.; Fitchett, D.; Bluhmki, E.; Hantel, S.; Mattheus, M.; Devins, T.; Johansen, O.E.; Woerle, H.J.; et al. Empagliflozin, Cardiovascular Outcomes, and Mortality in Type 2 Diabetes. *N. Engl. J. Med.* **2015**, *373*, 2117–2128. [[CrossRef](#)]
16. Perkovic, V.; Jardine, M.J.; Neal, B.; Bompoint, S.; Heerspink, H.J.L.; Charytan, D.M.; Edwards, R.; Agarwal, R.; Bakris, G.; Bull, S.; et al. Canagliflozin and Renal Outcomes in Type 2 Diabetes and Nephropathy. *N. Engl. J. Med.* **2019**, *380*, 2295–2306. [[CrossRef](#)]
17. Heerspink, H.J.L.; Stefánsson, B.V.; Correa-Rotter, R.; Chertow, G.M.; Greene, T.; Hou, F.-F.; Mann, J.F.E.; McMurray, J.J.V.; Lindberg, M.; Rossing, P.; et al. Dapagliflozin in Patients with Chronic Kidney Disease. *N. Engl. J. Med.* **2020**, *383*, 1436–1446. [[CrossRef](#)]
18. The EMPA-KIDNEY Collaborative Group. Empagliflozin in Patients with Chronic Kidney Disease. *N. Engl. J. Med.* **2023**, *388*, 117–127. [[CrossRef](#)]
19. Kristensen, S.L.; Rørth, R.; Jhund, P.S.; Docherty, K.F.; Sattar, N.; Preiss, D.; Køber, L.; Petrie, M.C.; McMurray, J.J.V. Cardiovascular, Mortality, and Kidney Outcomes with GLP-1 Receptor Agonists in Patients with Type 2 Diabetes: A Systematic Review and Meta-Analysis of Cardiovascular Outcome Trials. *Lancet Diabetes Endocrinol.* **2019**, *7*, 776–785. [[CrossRef](#)]
20. Filippatos, G.; Anker, S.D.; Agarwal, R.; Ruilope, L.M.; Rossing, P.; Bakris, G.L.; Tasto, C.; Joseph, A.; Kolkhof, P.; Lage, A.; et al. Finerenone Reduces Risk of Incident Heart Failure in Patients With Chronic Kidney Disease and Type 2 Diabetes: Analyses From the FIGARO-DKD Trial. *Circulation* **2022**, *145*, 437–447. [[CrossRef](#)]
21. Ruilope, L.M.; Pitt, B.; Anker, S.D.; Rossing, P.; Kovesdy, C.P.; Pecoits-Filho, R.; Pergola, P.; Joseph, A.; Lage, A.; Mentenich, N.; et al. Kidney Outcomes with Finerenone: An Analysis from the FIGARO-DKD Study. *Nephrol. Dial. Transplant.* **2023**, *38*, 372–383. [[CrossRef](#)]
22. Rebelos, E.; Tentolouris, N. Complementary Actions of Finerenone and SGLT2-i on Renal Outcomes?: An Urgent Need for More Information. *Nephrology* **2022**, *27*, 915–916. [[CrossRef](#)]
23. Selby, N.M.; Blankestijn, P.J.; Boor, P.; Combe, C.; Eckardt, K.-U.; Eikefjord, E.; Garcia-Fernandez, N.; Golay, X.; Gordon, I.; Grenier, N.; et al. Magnetic Resonance Imaging Biomarkers for Chronic Kidney Disease: A Position Paper from the European Cooperation in Science and Technology Action PARENCHIMA. *Nephrol. Dial. Transplant.* **2018**, *33*, ii4–ii14. [[CrossRef](#)]
24. Mendichovszky, I.; Pullens, P.; Dekkers, I.; Nery, F.; Bane, O.; Pohlmann, A.; de Boer, A.; Ljimani, A.; Odudu, A.; Buchanan, C.; et al. Technical Recommendations for Clinical Translation of Renal MRI: A Consensus Project of the Cooperation in Science and Technology Action PARENCHIMA. *Magn. Reson. Mater. Phys. Biol. Med.* **2020**, *33*, 131–140. [[CrossRef](#)] [[PubMed](#)]
25. Grist, J.T.; Hansen, E.S.; Zöllner, F.G.; Laustsen, C. Sodium (^{23}Na) MRI of the Kidney: Basic Concept. In *Methods in Molecular Biology*; Humana Press: Totowa, NJ, USA, 2021; Volume 2216, pp. 257–266. [[CrossRef](#)]
26. Laustsen, C. Hyperpolarized Renal Magnetic Resonance Imaging: Potential and Pitfalls. *Front. Physiol.* **2016**, *7*, 72. [[CrossRef](#)]
27. Evans, R.G.; Gardiner, B.S.; Smith, D.W.; O'Connor, P.M. Intrarenal Oxygenation: Unique Challenges and the Biophysical Basis of Homeostasis. *Am. J. Physiol. Renal Physiol.* **2008**, *295*, F1259–F1270. [[CrossRef](#)] [[PubMed](#)]
28. Leong, C.-L.; Anderson, W.P.; O'Connor, P.M.; Evans, R.G. Evidence That Renal Arterial-Venous Oxygen Shunting Contributes to Dynamic Regulation of Renal Oxygenation. *Am. J. Physiol. Renal Physiol.* **2007**, *292*, F1726–F1733. [[CrossRef](#)] [[PubMed](#)]
29. Toth, G.B.; Varallyay, C.G.; Horvath, A.; Bashir, M.R.; Choyke, P.L.; Daldrup-Link, H.E.; Dosa, E.; Finn, J.P.; Gahramanov, S.; Harisinghani, M.; et al. Current and Potential Imaging Applications of Ferumoxytol for Magnetic Resonance Imaging. *Kidney Int.* **2017**, *92*, 47–66. [[CrossRef](#)]
30. Odudu, A.; Nery, F.; Harteveld, A.A.; Evans, R.G.; Pendse, D.; Buchanan, C.E.; Francis, S.T.; Fernández-Seara, M.A. Arterial Spin Labelling MRI to Measure Renal Perfusion: A Systematic Review and Statement Paper. *Nephrol. Dial. Transplant.* **2018**, *33*, ii15–ii21. [[CrossRef](#)]
31. Nery, F.; Gordon, I.; Thomas, D.L. Non-Invasive Renal Perfusion Imaging Using Arterial Spin Labeling MRI: Challenges and Opportunities. *Diagnostics* **2018**, *8*, 2. [[CrossRef](#)]
32. Nery, F.; Buchanan, C.E.; Harteveld, A.A.; Odudu, A.; Bane, O.; Cox, E.F.; Derlin, K.; Gach, H.M.; Golay, X.; Gutberlet, M.; et al. Consensus-Based Technical Recommendations for Clinical Translation of Renal ASL MRI. *Magn. Reson. Mater. Phys. Biol. Med.* **2020**, *33*, 141–161. [[CrossRef](#)]
33. Echeverria-Chasco, R.; Vidorreta, M.; Aramendía-Vidaurreta, V.; Cano, D.; Escalada, J.; Garcia-Fernandez, N.; Bastarrika, G.; Fernández-Seara, M.A. Optimization of Pseudo-Continuous Arterial Spin Labeling for Renal Perfusion Imaging. *Magn. Reson. Med.* **2021**, *85*, 1507–1521. [[CrossRef](#)] [[PubMed](#)]
34. Pruijm, M.; Milani, B.; Pivin, E.; Podhajska, A.; Vogt, B.; Stuber, M.; Burnier, M. Reduced Cortical Oxygenation Predicts a Progressive Decline of Renal Function in Patients with Chronic Kidney Disease. *Kidney Int.* **2018**, *93*, 932–940. [[CrossRef](#)]
35. Pruijm, M.; Mendichovszky, I.A.; Liss, P.; van der Niepen, P.; Textor, S.C.; Lerman, L.O.; Krediet, C.T.P.; Caroli, A.; Burnier, M.; Prasad, P.V. Renal Blood Oxygenation Level-Dependent Magnetic Resonance Imaging to Measure Renal Tissue Oxygenation: A Statement Paper and Systematic Review. *Nephrol. Dial. Transplant.* **2018**, *33*, ii22–ii28. [[CrossRef](#)] [[PubMed](#)]
36. Prasad, P.V.; Li, L.-P.; Thacker, J.M.; Li, W.; Hack, B.; Kohn, O.; Sprague, S.M. Cortical Perfusion and Tubular Function as Evaluated by Magnetic Resonance Imaging Correlates with Annual Loss in Renal Function in Moderate Chronic Kidney Disease. *Am. J. Nephrol.* **2019**, *49*, 114–124. [[CrossRef](#)]
37. Zanchi, A.; Burnier, M.; Muller, M.-E.; Ghajarzadeh-Wurzner, A.; Maillard, M.; Loncle, N.; Milani, B.; Dufour, N.; Bonny, O.; Pruijm, M. Acute and Chronic Effects of SGLT2 Inhibitor Empagliflozin on Renal Oxygenation and Blood Pressure Control in Nondiabetic Normotensive Subjects: A Randomized, Placebo-Controlled Trial. *J. Am. Heart Assoc.* **2020**, *9*, e016173. [[CrossRef](#)]

38. Laursen, J.C.; Søndergaard-Heinrich, N.; de Melo, J.M.L.; Haddock, B.; Rasmussen, I.K.B.; Safavimanesh, F.; Hansen, C.S.; Størling, J.; Larsson, H.B.W.; Groop, P.-H.; et al. Acute Effects of Dapagliflozin on Renal Oxygenation and Perfusion in Type 1 Diabetes with Albuminuria: A Randomised, Double-Blind, Placebo-Controlled Crossover Trial. *EClinicalMedicine* **2021**, *37*, 100895. [[CrossRef](#)] [[PubMed](#)]
39. Gullaksen, S.; Vernstrøm, L.; Sørensen, S.S.; Ringgaard, S.; Laustsen, C.; Funck, K.L.; Poulsen, P.L.; Laugesen, E. Separate and Combined Effects of Semaglutide and Empagliflozin on Kidney Oxygenation and Perfusion in People with Type 2 Diabetes: A Randomised Trial. *Diabetologia* **2023**, *66*, 813–825. [[CrossRef](#)] [[PubMed](#)]
40. Grenier, N.; Cornelis, F.; Le Bras, Y.; Rigou, G.; Boutault, J.R.; Bouzgarrou, M. Perfusion Imaging in Renal Diseases. *Diagn. Interv. Imaging* **2013**, *94*, 1313–1322. [[CrossRef](#)]
41. Green, M.A.; Hutchins, G.D. Positron Emission Tomography (PET) Assessment of Renal Perfusion. *Semin. Nephrol.* **2011**, *31*, 291–299. [[CrossRef](#)]
42. Juillard, L.; Janier, M.F.; Fouque, D.; Cinotti, L.; Maakel, N.; Le Bars, D.; Barthez, P.Y.; Pozet, N.; Laville, M. Dynamic Renal Blood Flow Measurement by Positron Emission Tomography in Patients with CRF. *Am. J. Kidney Dis.* **2002**, *40*, 947–954. [[CrossRef](#)]
43. Alpert, N.M.; Rabito, C.A.; Correia, D.J.A.; Babich, J.W.; Littman, B.H.; Tompkins, R.G.; Rubin, N.T.; Rubin, R.H.; Fischman, A.J. Mapping of Local Renal Blood Flow with PET and H₂¹⁵O. *J. Nucl. Med.* **2002**, *43*, 470–475.
44. Päivärinta, J.; Oikonen, V.; Räisänen-Sokolowski, A.; Tolvanen, T.; Löyttyniemi, E.; Iida, H.; Nuutila, P.; Metsärinne, K.; Koivuvuuta, N. Renal Vascular Resistance Is Increased in Patients with Kidney Transplant. *BMC Nephrol.* **2019**, *20*, 437. [[CrossRef](#)] [[PubMed](#)]
45. Nitzsche, E.U.; Choi, Y.; Killion, D.; Hoh, C.K.; Hawkins, R.A.; Rosenthal, J.T.; Buxton, D.B.; Huang, S.C.; Phelps, M.E.; Schelbert, H.R. Quantification and Parametric Imaging of Renal Cortical Blood Flow in Vivo Based on Patlak Graphical Analysis. *Kidney Int.* **1993**, *44*, 985–996. [[CrossRef](#)] [[PubMed](#)]
46. Normand, G.; Lemoine, S.; Le Bars, D.; Merida, I.; Irace, Z.; Troalen, T.; Costes, N.; Juillard, L. PET [¹¹C]Acetate Is Also a Perfusion Tracer for Kidney Evaluation Purposes. *Nucl. Med. Biol.* **2019**, *76–77*, 10–14. [[CrossRef](#)]
47. Tahari, A.K.; Bravo, P.E.; Rahmim, A.; Bengel, F.M.; Szabo, Z. Initial human experience with Rubidium-82 renal PET/CT imaging. *J. Med. Imaging Radiat. Oncol.* **2014**, *58*, 25–31. [[CrossRef](#)]
48. Koivuvuuta, N.; Liukko, K.; Kudomi, N.; Oikonen, V.; Tertti, R.; Manner, I.; Vahlberg, T.; Nuutila, P.; Metsärinne, K. The Effect of Revascularization of Renal Artery Stenosis on Renal Perfusion in Patients with Atherosclerotic Renovascular Disease. *Nephrol. Dial. Transplant.* **2012**, *27*, 3843–3848. [[CrossRef](#)] [[PubMed](#)]
49. Assersen, K.B.; Høilund-Carlsen, P.F.; Olsen, M.H.; Greve, S.V.; Gam-Hadberg, J.C.; Braad, P.-E.; Damkjaer, M.; Bie, P. The Exaggerated Natriuresis of Essential Hypertension Occurs Independently of Changes in Renal Medullary Blood Flow. *Acta Physiol.* **2019**, *226*, e13266. [[CrossRef](#)]
50. Rebelos, E.; Dadson, P.; Oikonen, V.; Iida, H.; Hannukainen, J.C.; Iozzo, P.; Ferrannini, E.; Nuutila, P. Renal Hemodynamics and Fatty Acid Uptake: Effects of Obesity and Weight Loss. *Am. J. Physiol. -Endocrinol. Metab.* **2019**, *317*, E871–E878. [[CrossRef](#)]
51. Middlekauff, H.R.; Nitzsche, E.U.; Hoh, C.K.; Hamilton, M.A.; Fonarow, G.C.; Hage, A.; Moriguchi, J.D. Exaggerated Muscle Mechanoreflex Control of Reflex Renal Vasoconstriction in Heart Failure. *J. Appl. Physiol.* **2001**, *90*, 1714–1719. [[CrossRef](#)]
52. Middlekauff, H.R.; Nitzsche, E.U.; Nguyen, A.H.; Hoh, C.K.; Gibbs, G.G. Modulation of Renal Cortical Blood Flow during Static Exercise in Humans. *Circ. Res.* **1997**, *80*, 62–68. [[CrossRef](#)]
53. Kudomi, N.; Koivuvuuta, N.; Liukko, K.E.; Oikonen, V.J.; Tolvanen, T.; Iida, H.; Tertti, R.; Metsärinne, K.; Iozzo, P.; Nuutila, P. Parametric Renal Blood Flow Imaging Using [¹⁵O]H₂O and PET. *Eur. J. Nucl. Med. Mol. Imaging* **2009**, *36*, 683–691. [[CrossRef](#)]
54. Damkjær, M.; Vafaee, M.; Møller, M.L.; Braad, P.E.; Petersen, H.; Høilund-Carlsen, P.F.; Bie, P. Renal Cortical and Medullary Blood Flow Responses to Altered NO Availability in Humans. *Am. J. Physiol. Integr. Comp. Physiol.* **2010**, *299*, R1449–55. [[CrossRef](#)] [[PubMed](#)]
55. Damkjær, M.; Vafaee, M.; Braad, P.E.; Petersen, H.; Høilund-Carlsen, P.F.; Bie, P. Renal Cortical and Medullary Blood Flow during Modest Saline Loading in Humans. *Acta Physiol.* **2012**, *205*, 472–483. [[CrossRef](#)]
56. Mather, A.; Pollock, C. Glucose Handling by the Kidney. *Kidney Int.* **2011**, *79*, S1–S6. [[CrossRef](#)]
57. Balaban, R.S.; Mandel, L.J. Metabolic Substrate Utilization by Rabbit Proximal Tubule. An NADH Fluorescence Study. *Am. J. Physiol.* **1988**, *254*, F407–F416. [[CrossRef](#)]
58. Rebelos, E.; Mari, A.; Oikonen, V.; Iida, H.; Nuutila, P.; Ferrannini, E. Evaluation of Renal Glucose Uptake with [¹⁸F]FDG-PET: Methodological Advancements and Metabolic Outcomes. *Metabolism* **2023**, *141*, 155382. [[CrossRef](#)] [[PubMed](#)]
59. Kessara, A.; Buyukcizmeci, N.; Gedik, G.K. Estimation of patient organ and Whole-Body Doses in [¹⁸F-FDG] PET/CT SCAN. *Radiat. Prot. Dosim.* **2023**, *199*, 61–68. [[CrossRef](#)] [[PubMed](#)]
60. Prasad, P.V.; Li, L.-P.; Hack, B.; Leloudas, N.; Sprague, S.M. Quantitative Blood Oxygenation Level Dependent Magnetic Resonance Imaging for Estimating Intra-Renal Oxygen Availability Demonstrates Kidneys Are Hypoxic in Human CKD. *Kidney Int. Rep.* **2023**, *8*, 1057–1067. [[CrossRef](#)]
61. Gooding, K.M.; Lienczewski, C.; Papale, M.; Koivuvuuta, N.; Maziarz, M.; Dutius Andersson, A.-M.; Sharma, K.; Pontrelli, P.; Garcia Hernandez, A.; Bailey, J.; et al. Prognostic Imaging Biomarkers for Diabetic Kidney Disease (IBEAT): Study Protocol. *BMC Nephrol.* **2020**, *21*, 242. [[CrossRef](#)]
62. Moriconi, D.; Nannipieri, M.; Dadson, P.; Rosada, J.; Tentolouris, N.; Rebelos, E. The Beneficial Effects of Bariatric-Surgery-Induced Weight Loss on Renal Function. *Metabolites* **2022**, *12*, 967. [[CrossRef](#)] [[PubMed](#)]

63. Moritz, E.; Dadson, P.; Saukko, E.; Honka, M.-J.; Koskensalo, K.; Seppälä, K.; Pekkarinen, L.; Moriconi, D.; Helmiö, M.; Salminen, P.; et al. Renal Sinus Fat Is Expanded in Patients with Obesity and/or Hypertension and Reduced by Bariatric Surgery Associated with Hypertension Remission. *Metabolites* **2022**, *12*, 617. [[CrossRef](#)] [[PubMed](#)]
64. Mancini, M.; Summers, P.; Faita, F.; Brunetto, M.R.; Callea, F.; de Nicola, A.; Di Lascio, N.; Farinati, F.; Gastaldelli, A.; Gridelli, B.; et al. Digital Liver Biopsy: Bio-Imaging of Fatty Liver for Translational and Clinical Research. *World J. Hepatol.* **2018**, *10*, 231–245. [[CrossRef](#)] [[PubMed](#)]
65. Mantovani, A.; Pelusi, S.; Margarita, S.; Malvestiti, F.; Dell’Alma, M.; Bianco, C.; Ronzoni, L.; Prati, D.; Targher, G.; Valenti, L. Adverse Effect of PNPLA3 p.I148M Genetic Variant on Kidney Function in Middle-Aged Individuals with Metabolic Dysfunction. *Aliment. Pharmacol. Ther.* **2023**, *57*, 1093–1102. [[CrossRef](#)] [[PubMed](#)]

Disclaimer/Publisher’s Note: The statements, opinions and data contained in all publications are solely those of the individual author(s) and contributor(s) and not of MDPI and/or the editor(s). MDPI and/or the editor(s) disclaim responsibility for any injury to people or property resulting from any ideas, methods, instructions or products referred to in the content.